SICE Journal of Control, Measurement, and System Integration, Vol. 7, No. 2, pp. 122–131, March 2014

An Improved Incremental Conductance-Maximum Power Point Tracking Algorithm Based on Fuzzy Logic for Photovoltaic Systems

Nguyen Gia Minh THAO *, Kenko UCHIDA *,**, and Nam NGUYEN-QUANG ***

Abstract: This paper presents an improved Incremental Conductance - Maximum Power Point Tracking (INC-MPPT) algorithm based on fuzzy logic for photovoltaic (PV) systems. The demonstrative PV system consists of the solar array with a nominal power of 320W, a non-inverting buck-boost converter, and a resistive load. The PV system's objective is to seek efficiently the maximum power point (MPP) of the solar array in varying weather conditions. To do this, the proposed fuzzy-based INC-MPPT algorithm is designed with two sub-controllers. Wherein, in the first one, a novel fuzzy logic controller (FLC) is proposed to enhance the effectiveness of the conventional INC-MPPT. Its aim is determining rapidly and accurately the optimal voltage, where the solar array operates at the MPP. The other is a PI anti-windup controller, and it regulates the operating PV array's voltage to the optimal voltage computed in advance. Simulations show that the suggested algorithm fulfills well the listed goal even when the solar irradiance and temperature change suddenly. Furthermore, comparisons of simulation results, obtained from the presented algorithm, the conventional INC, and an existing fuzzy-based INC-MPPT, illustrate advantages of the proposed algorithm in terms of fast response speed, high accuracy, and small oscillation. The feasibility and efficacy of the suggested algorithm are also verified by experiments.

Key Words: PV system, INC-MPPT algorithm, fuzzy logic, PI anti-windup, non-inverting buck-boost converter.

1. Introduction

Nowadays, the use of renewable-energy sources is an advance in many countries when the fossil-fuel resources are going to be exhausted, and the environment protection is an important issue [1]. In which, the solar energy is one of those sources with outstanding features such as an unlimited power and environmentally friendly resource [2]. Therefore, PV systems are now playing an ever-increasingly significant role in supplying electric power in the recent years. According to [1],[2], PV systems commonly have two modes in operation; that is the stand-alone PV system and the grid-connected PV system. In detail, the stand-alone PV system often uses battery banks to store the energy obtained from solar panels, and its operation is independent of the electric grid. Whereas, the grid-connected PV system is normally used in distributed generation systems to deliver the power to the utility grid.

Referring in [3], in a PV system, to obtain the power from PV panels efficiently, two key factors should be examined thoroughly. Namely, the first one is impacts of the weather parameters. Another is effects of power-electronic converters, controllers and loads utilized in the designed PV system. Obviously, the weather condition is out of the user's control. Thus, the converters in use must be controlled effectively to maximize the output power. According to [4], there are many dissimilar MPPT algorithms have been introduced with varying the complexity, response speed, accuracy, adaptability, and cost.

* Department of Electrical Engineering and Bioscience, Waseda University, Tokyo 169-8555, Japan.
** JST-CREST, Tokyo 169–8555, Japan.
*** Faculty of Electrical and Electronics Engineering, Ho Chi Minh City University of Technology, Vietnam.
E-mail: thao@uchi.elec.waseda.ac.jp
(Received September 19, 2013)

Wherein, Perturb and Observe (P&O) is known as the most popular algorithm used in commercial products [1],[4]. In detail, they use the slope of the power-voltage (P-V) curve, $(\Delta P_P/\Delta V_P)$, to track the MPP. However, they make large fluctuations around the MPP, and fail to determine the new MPP of the PV panels when weather parameters drastically change [1]. Another common MPPT method is the Fractional Open-Circuit Voltage. This algorithm assigns the ratio of the optimal voltage V_{MPP} to the open-circuit voltage V_{OC} as a constant K_{MPP}, ($V_{MPP} = K_{MPP} \times V_{OC}$; Fig. 6). Then the DC-DC converter is controlled to force the operating PV panel's voltage to be equal to V_{MPP} for reaching the MPP. Referring in [4], the constant K_{MPP} often has value in the interval (0.71 0.78). Nevertheless, it is too difficult to choose exactly the optimal value for K_{MPP}, since characteristics of PV panel are highly nonlinear and affected by changes of weather parameters.

According to [2],[4] and Fig. 6, the INC-MPPT algorithm uses the ratio-value between the slope of P-V curve and the PV panel's voltage, $C_P = (\Delta P_P/\Delta V_P)/V_P = \Delta I_P/V_P + \Delta I_P/\Delta V_P$, to seek the MPP. In detail, the ratio-value is zero at the MPP, negative on the right side and positive on the left side of MPP. The INC-MPPT algorithm is also widely used due to its high accuracy in tracing the MPP. Furthermore, this method is fairly simple and easy to implement. However, in the technique, the step-size $\Delta V(k)$ is a fixed value; and is often adjusted to being small enough to capture the MPP accurately and reduce the oscillation around the MPP [2]. Therefore, the response time of this method is relatively long, especially when the weather condition changes suddenly.

To overcome the listed major disadvantage and elevate the effectiveness of the conventional INC-MPPT method, many techniques have been introduced in [2],[4]–[14]. The main purpose of those improved INC-MPPT algorithms is to make the step-

size be variable. Referring in [2], the step-size is changed adaptively according to the slope of the P-V curve ($\Delta P_P/\Delta V_P$). In detail, the step-size will be tiny when ($\Delta P_P/\Delta V_P$) becomes very small to avoid oscillating around the MPP. Hence, this method has a good steady-state response. Nevertheless, when the solar radiation drastically varies, ($\Delta P_P/\Delta V_P$) becomes huge, and this will cause the step-size to be very large in a short transient-time [5]. Therefore, dynamic characteristics of the PV system in use may be not stable in this condition. The authors in [5] presented a modified variable step-size INC-MPPT based on the current-mode control. This method not only improves the response speed in seeking the MPP but also reduces the steady-state fluctuations around the MPP. However, its design structure is quite complex to implement into experimental PV systems.

On the other hand, the FLC has been proposed to enhance the performance of the conventional INC-MPPT [6]–[14]. According to [6] and [7], in most of the existing fuzzy-based INC-MPPT techniques, the ratio-value ($I_P/V_P + \Delta I_P/\Delta V_P$) and its change are used to search the MPP. However, in those methods, the operating point of PV panel may move away far from the MPP when the solar radiation varies abruptly, because the change of the step-size is disregarded. In addition, the authors in [8] introduced a FLC with the power variation $\Delta P_P(k)$ and the previous value of duty-cycle $u(k-1)$ as two inputs; and the FLC's output is the duty-cycle value $u(k)$. This algorithm ameliorates the dynamic characteristics in reaching the MPP under weather variations. Nevertheless, in the performance of the method, the oscillation around the MPP occurs at the steady state. Besides, a self-organizing FLC for MPPT based on the Look-up-Table method, is described in [9]. The response of the method is pretty good, but is affected by the technique utilized to set and update values in the reference tables. Referring in [10], fuzzy cognitive networks are supplemented to elevate the response speed in seeking the MPP. As a result, the response speed of this algorithm is faster than the ordinary fuzzy-based MPPT in [6]. Nonetheless, the technique needs a specialized sensor to calculate the short-circuit current of PV panels.

In this research, an ameliorated INC-MPPT algorithm based on fuzzy logic for stand-alone PV systems is proposed. Therein, a novel FLC is designed to boost the effectiveness of the conventional INC-MPPT, especially in improving the response speed and reducing fluctuations around the MPP. In detail, from the absolute value of a modified ratio-value and the previous step-size $\Delta V(k-1)$, the proposed FLC, comprising 25 fuzzy rules, adjusts suitably the step-size $\Delta V(k)$ to determine speedily and exactly the optimal voltage V_{MPP} (see Figs. 7 and 8). Simulations and experimental results, including the consideration on impacts of the weather parameters, are shown to assess the effectiveness of the suggested algorithm.

The remainder of this paper is organized as follows. Section 2 shows the description of demonstrative PV system. Design steps of the proposed fuzzy-based algorithm are presented in the next section. Simulation results of the closed-loop control system are illustrated in Section 4. This section also describes the comparisons between the suggested algorithm, the conventional INC in [4] and the conventional fuzzy-based INC-MPPT in [6]. Section 5 shows the efficacy of the proposed method in experiments. The conclusion and the direction for future development of this study are given in Section 6. Two last parts are respectively the acknowledgment and the references.

2. Demonstrative PV System

2.1 Demonstrative PV System Description

Referring in [5]–[15], many different kinds of DC-DC converter have been used in PV systems such as Buck, Boost, Cuk, Sepic, etc. In this study, the non-inverting buck-boost converter introduced in [16] is utilized for the demonstrative PV system.

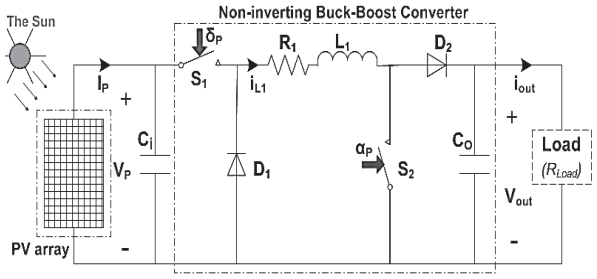

Fig. 1 The demonstrative PV system used in this study.

Table 1 Some variables of the demonstrative PV system.

Variable (see Fig. 1)	**Symbol**
PV array's voltage	V_P
PV array's current	I_P
Input binary control signals of buck-boost converter	δ_p and α_p

As seen in Fig. 1, the illustrative PV system consists of the PV array with a nominal power of 320W, the non-inverting buck-boost converter, and a resistive load. The electric energy is transferred from the PV array to the buck-boost converter, and then supplies for the load. As given by Table 1, switches S_1 and S_2 are activated by the binary control signals δ_p and α_p respectively. According to [16] and [17], the advantages of this buck-boost converter are it has the non-inverting output, and can be driven to operate in three different modes. In detail,

- *Buck-Boost* mode: In this case, the switches S_1 and S_2 are synchronously activated as follows:

$$\alpha_p = \delta_p = \begin{cases} 0, & S_1 \text{ and } S_2 \text{ are OFF} \\ 1, & S_1 \text{ and } S_2 \text{ are ON} \end{cases}$$

- *Buck* mode: In this condition, the switch S_2 is always OFF ($\alpha_p = 0$); meanwhile, S_1 is activated by δ_p as follows:

$$\delta_p = \begin{cases} 0, & S_1 \text{ is OFF} \\ 1, & S_1 \text{ is ON} \end{cases}$$

- *Boost* mode: In this situation, the switch S_1 is always ON ($\delta_p = 1$); meanwhile, S_2 is activated by α_p as follows:

$$\alpha_p = \begin{cases} 0, & S_2 \text{ is OFF} \\ 1, & S_2 \text{ is ON} \end{cases}$$

2.2 PV Panel Model

According to [1],[18], the equivalent circuit of a PV cell and model of a PV panel are shown in Fig. 2 and (1), respectively.

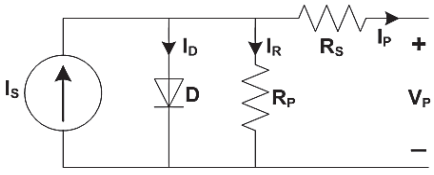

Fig. 2 The equivalent circuit for a PV cell.

$$I_P = N_P I_S - N_P I_O\left[\mathrm{e}\left\{\frac{q(V_P + R_S I_P)}{N_S akT}\right\} - 1\right] - N_P\left(\frac{V_P + R_S I_P}{N_S R_P}\right). \quad (1)$$

$$I_S(T,G) = \left[I_{SC,n} + k_T(T - T_n)\right]\frac{G}{G_n}. \quad (2)$$

$$I_O(T) = \left[\frac{I_{SC,n}}{\mathrm{e}\left\{\frac{qV_{OC,n}}{N_S akT_n}\right\} - 1}\right]\left(\frac{T}{T_n}\right)^3 \mathrm{e}\left\{\frac{qE_g}{ak}\left(\frac{1}{T_n} - \frac{1}{T}\right)\right\}. \quad (3)$$

I_S is the photoelectric current related to the solar radiation; I_O is the saturation diode current; q is the electric charge, 1.602×10^{-19} C; k is the Boltzmann's constant, 1.381×10^{-23} J/K; a is the diode ideality constant and its value is in the interval [1 2], 1.6; E_g is the energy gap of the material used to make the solar cell, 1.12 eV; k_T is the temperature coefficient; N_S and N_P are the number of PV cells in series and parallel respectively in the PV panel; G and $G_n = 1000$ W/m^2, are the solar irradiance at the operating condition and standard condition, respectively; T and $T_n = 298$ K, are the absolute temperatures (in Kelvin degree) of the PV cell at the operating condition and the standard condition, respectively; $I_{SC,n}$ and $V_{OC,n}$ are the short-circuit current and the open-circuit voltage of the PV panel at the standard condition, respectively.

In this study, the *BP-380J* 80W PV panel in [19] is used. In detail, Table 2 shows its characteristics at the standard test condition, where $G = G_n = 1000$ W/m^2, $T = T_n = 298$ K = 25°C. Effects of solar irradiance and temperature to the PV panel are represented in Figs. 3 and 4, respectively. As shown in Table 3, the PV array in Fig. 1 comprises two parallel branches with two the *BP-380J* PV panels in series in each branch.

3. Proposed Fuzzy-Based INC-MPPT Algorithm

The key goal of the designed PV system is to obtain optimally the electric energy from the PV array in varying weather conditions. As shown in Fig. 5, the proposed algorithm consists of two the major sub-controllers as follows:

- The first is an ameliorated INC-MPPT method using a novel FLC. From the PV array's voltage and current, it calculates the reference voltage $V_{MPP}^{ref}(k)$, where the PV array operates at the MPP (see Fig. 6). Let us emphasize that the proposed FLC in this sub-controller is the most important part of the suggested INC-MPPT algorithm.
- Another is a PI controller, including an anti-windup block. It controls the converter to ensure that the PV array's voltage $V_P(k)$ must be closely equal to $V_{MPP}^{ref}(k)$ computed beforehand by the first sub-controller.

Table 2 Characteristics of the *BP-380J* PV panel [19].

Parameter	Symbol	Value
Maximum (peak) output power	P_P^{max}	80 W
Voltage at the MPP	V_{MPP}	17.6 V
Current at the MPP	I_{MPP}	4.5 A
Open-circuit voltage	V_{OC}	22.1 V
Short-circuit current	I_{SC}	4.8 A
Number of cells in series, parallel	N_S, N_P	36, 1

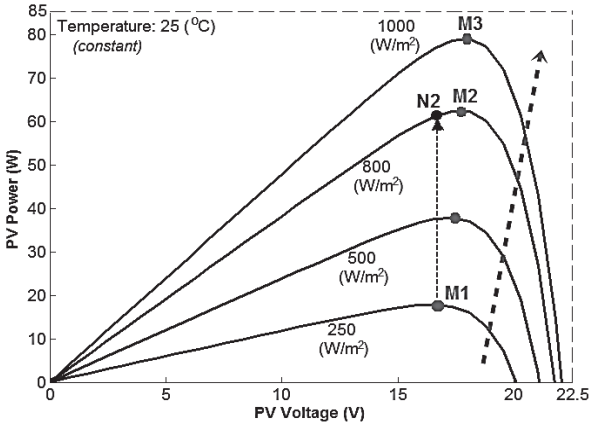

Fig. 3 Effect of solar radiation changes to the *BP-380J* PV panel.

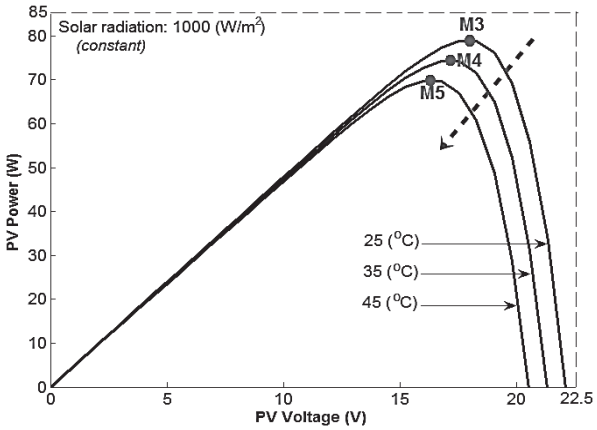

Fig. 4 Impact of temperature variations to the *BP-380J* PV panel.

Table 3 Values of the MPPs shown in Fig. 3 and Fig. 4.

a PV panel	M1	M2	M3	M4	M5
$V_{P,panel}$ (V)	16.49	17.46	17.65	16.94	16.1
$P_{P,panel}$ (W)	18.28	63.3	80	75.3	70.85
PV array	**M1**	**M2**	**M3**	**M4**	**M5**
V_P (V)	32.98	34.92	35.3	33.88	32.2
P_P (W)	73.12	253.2	320	301.2	283.4

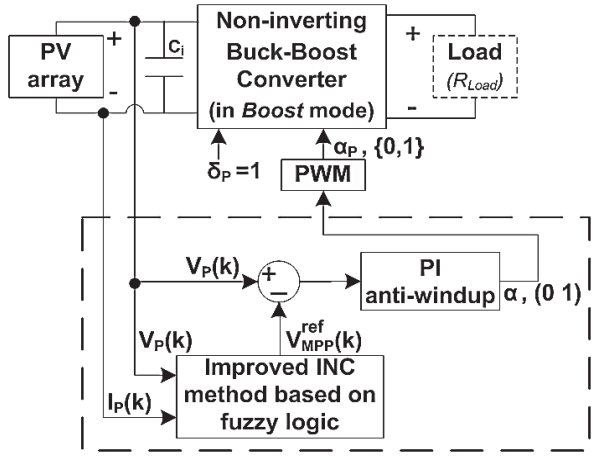

Fig. 5 The structure of the proposed algorithm.

Besides, as seen in Fig. 5, the designed buck-boost converter is now controlled to operate in *Boost* mode.

3.1 The First Sub-Controller

As presented in Fig. 7, this sub-controller is a modified INC-MPPT method based on fuzzy logic. Wherein, the proposed FLC adjusts appropriately the step-size $\Delta V(k)$ for improving

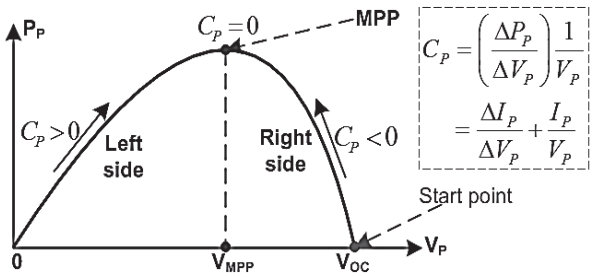

Fig. 6 The power-voltage (P-V) curve of the PV array.

the response speed in seeking the MPP and eliminating oscillations around the MPP. As seen in Fig. 8, the FLC is designed with two inputs and one output. In detail, the first input of the FLC is the absolute value of a modified ratio-value $|A_P(k)|$, including a scaling factor g_1, where $A_P(k)$ is expressed in (5); or is the absolute value of PV current's change $|\Delta I_P(k)|$, where $\Delta I_P(k)$ is given by (7). The other input is the previous value of the step-size $\Delta V(k-1)$. The FLC's output is the additional value $V_{Add}(k)$ utilized to tune adaptively the step-size $\Delta V(k)$. Obviously, the main aim of the suggested FLC is to make the step-size $\Delta V(k)$ to be a variable value, instead of the fixed value in the conventional INC-MPPT method. Figures 7 and 8 illustrate the detailed flowchart of the proposed algorithm.

$$P_P(k) = V_P(k)I_P(k). \tag{4}$$

$$A_P(k) = g_1 C_P(k) = g_1\left[\frac{\Delta I_P(k)}{\Delta V_P(k)} + \frac{I_P(k)}{V_P(k)}\right]. \tag{5}$$

Where g_1 is a positive value, and is used to enhance the sensitivity of the ratio-value $C_P(k)$.

$$\Delta V_P(k) = V_P(k) - V_P(k-1). \tag{6}$$

$$\Delta I_P(k) = I_P(k) - I_P(k-1). \tag{7}$$

As can be seen in Fig. 7, in the condition "$\Delta V_P(k) = 0$ and $\Delta I_P(k) \neq 0$", the first FLC's input is chosen as $|\Delta I_P(k)|$. Let us note that this case is only utilized in a special time-period when the weather parameters change suddenly.

For example, as shown in Fig. 3, if the solar radiation increases abruptly from 250 W/m^2 to 800 W/m^2, the operating power point of the PV panel will move instantly from the point M1 to the point N2. Meanwhile, the PV panel's voltage does not change in this transient time-period, and it means that $\Delta V_P(k) = 0$. Furthermore, it is clearly to see that M1 is the MPP where the solar irradiance is 250 W/m^2, but N2 is not the MPP where the solar radiation is 800 W/m^2. Therefore, in the moving time-period from the point M1 to the point N2, $|\Delta I_P(k)|$ is chosen as the first input of FLC. Then, when $\Delta V_P(k) \neq 0$, the first FLC's input is switched to be $|A_P(k)|$ for forcing the operating power point from the point N2 to reach the new MPP M2 (see Figs. 3 and 7).

In addition, unexpected big variations of the step-size may cause fluctuations in the PV output power at the steady state. Thus, a switching module is proposed to eliminate this inconvenience thoroughly as shown in Fig. 8. Based on the value of the input, $|A_P(k)|$ or $|\Delta I_P(k)|$, the suggested module assigns a suitable value for the output scaling coefficient g_2. Table 4 shows the operation of the switching module.

3.1.1 Fuzzification

Two inputs: have same five linguistic variables, the membership function, and value in the interval [0 1].

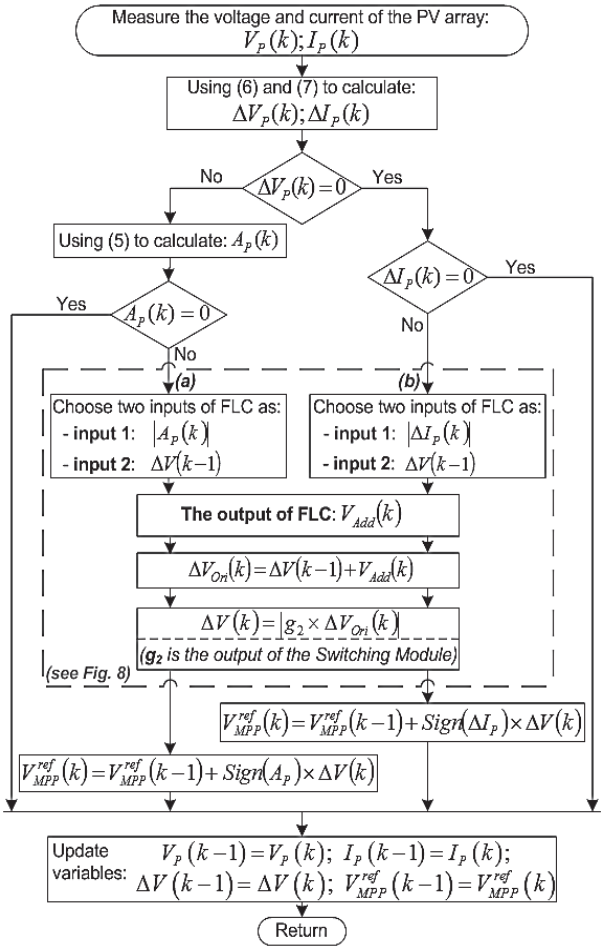

Fig. 7 The detailed flowchart of the proposed method.

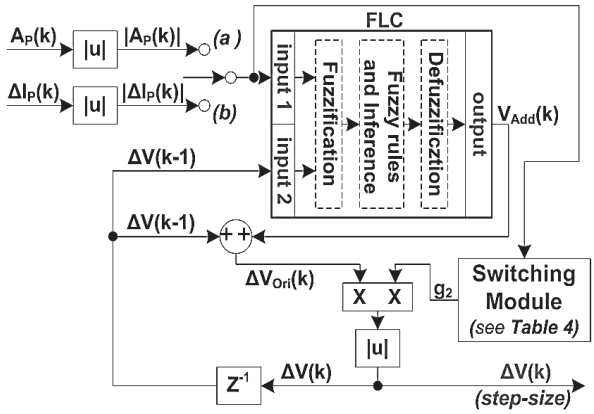

Fig. 8 The particular scheme of the proposed FLC.

Table 4 Operation of the Switching Module in Fig. 8.

(**a**)	$\frac{\lvert A_P(k)\rvert}{g_1} \geq 0.05$	$\frac{\lvert A_P(k)\rvert}{g_1} < 0.05$
If the input is $\lvert A_P(k)\rvert$	$g_2 = 1$	$g_2 = 0.34$
(**b**) If the input is $\lvert \Delta I_P(k)\rvert$	$g_2 = 1$ (where every value of $\lvert \Delta I_P(k)\rvert$)	

- $|A_P(k)|$ or $|\Delta I_P(k)|$ = [Very Small, Small, Medium, Large, Very Large]
  = [VS, SM, ME, LA, VL]
- $\Delta V(k-1)$ = [Very Small, Small, Medium, Large, Very Large]
  = [VS, SM, ME, LA, VL]

The output: has nine linguistic variables and the value in the interval [−1 1].

$V_{Add}(k)$ = [Negative Large, Negative Medium, Negative Small, Negative Zero, Zero, Positive Zero, Positive Small, Positive Medium, Positive Large]
= [NL, NM, NS, NZ, ZE, PZ, PS, PM, PL]

Membership functions:

The membership functions for two inputs and the output of the FLC are described in Figs. 9 and 10, respectively.

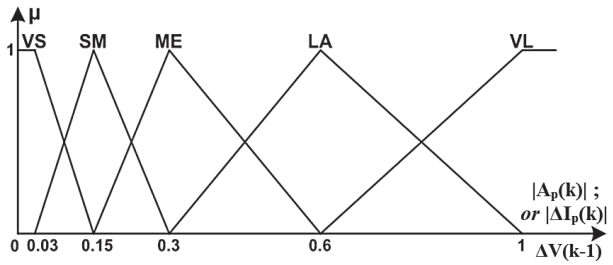

Fig. 9 The membership function for two inputs of FLC.

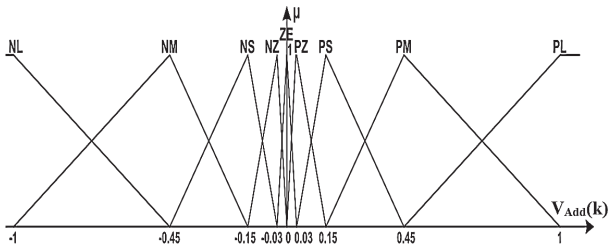

Fig. 10 The membership function for the output of FLC.

3.1.2 Fuzzy association rules

The fuzzy associative matrix is illustrated by Table 5. It is represented in the form "**if** ... **then** ...", and totally has 5×5 = 25 rules. Wherein, a sample fuzzy rule is expressed as follows: **if** $|A_P(k)|$ is VL and $\Delta V(k-1)$ is VS **then** $V_{Add}(k)$ is PL.

The design technique for the fuzzy association rules is mainly based on the authors' knowledge and experiences in the PV system. Moreover, in this study, the designed association rules and membership functions have been already optimized by the trial-and-error method.

Interpretation for the fuzzy association rules:

According to Figs. 7 and 8, if $\Delta V_P(k) \neq 0$ and $A_P(k) \neq 0$, the first FLC's input is chosen as $|A_P(k)|$, the absolute value of the modified ratio-value. As seen in Table 5 and Fig. 6, if $|A_P(k)|$ is VL (very large), we can predict that the operating point of PV array may be on the left side or the right side of the P-V curve, where is very far from the MPP. Meanwhile, as shown in Table 5, the second FLC's input $\Delta V(k-1)$, the previous value of step-size, is a value in five following cases: VS, SM, ME, LA and VL.

In detail, firstly, if $\Delta V(k-1)$ is VS (very small), it means that the step-size must be summed with a big positive value to force the operating point to move to the MPP quickly. So the additional value for the step-size, $V_{Add}(k)$, needs to be assigned as PL (positive large). Similarly, if $\Delta V(k-1)$ is SM (small), $V_{Add}(k)$ can be chosen as PM (positive medium) to reach the MPP speedily. Otherwise, if $\Delta V(k-1)$ is ME (medium), it is easy to see that the step-size should be added a small positive value to achieve the MPP without the oscillation around it. Therefore, $V_{Add}(k)$ has to be PS (positive small). Lastly, if $\Delta V(k-1)$ is LA (large) or VL (very large), this means that the operating point has the tendency in automatically reaching the MPP. Hence, $V_{Add}(k)$ must be PZ (positive zero) or ZE (zero) respectively to avoid surpassing the MPP in the opposite side for eliminating fluctuations. In general, the similar deductive way can be used to interpret for the other fuzzy associative rules described in Table 5.

Table 5 The fuzzy association rules of the proposed FLC.

$\mathbf{V_{Add}(k)}$		$\mathbf{\lvert A_P(k)\rvert}$ *or* $\mathbf{\lvert \Delta I_P(k)\rvert}$				
		VS	SM	ME	LA	VL
$\Delta\mathbf{V(k-1)}$	VS	ZE	PZ	PS	PM	PL
	SM	NZ	ZE	PZ	PS	PM
	ME	NS	NZ	ZE	PZ	PS
	LA	NM	NS	NZ	ZE	PZ
	VL	NL	NM	NS	NZ	ZE

On the other hand, if the first FLC's input is defined as $A_P(k)$ or $\Delta I_P(k)$ (instead of $|A_P(k)|$ or $|\Delta I_P(k)|$, respectively), which has ten linguistic variables in both negative and positive values, the fuzzy associative matrix will have $10 \times 5 = 50$ rules. However, this 50-rule FLC has the same control cases (the same control quality) as the suggested 25-rule FLC shown in Table 5, where $|A_P(k)|$ or $|\Delta I_P(k)|$ is utilized as the first FLC's input. Thus, the design technique for the 25-rule FLC helps reduce fifty percent of the quantity of fuzzy association rules (from 50 rules to 25 rules) to elevate the feasibility of the proposed method.

3.1.3 Fuzzy rule inference and defuzzification

In this paper, the max-minimum operation and the centroid (center of area) technique [20] are used for the fuzzy rule inference and the defuzzification, respectively. In detail, the design of the fuzzy rule inference and defuzzification, based on the Fuzzy Inference System (FIS) editor of Matlab software, is described in Fig. 11.

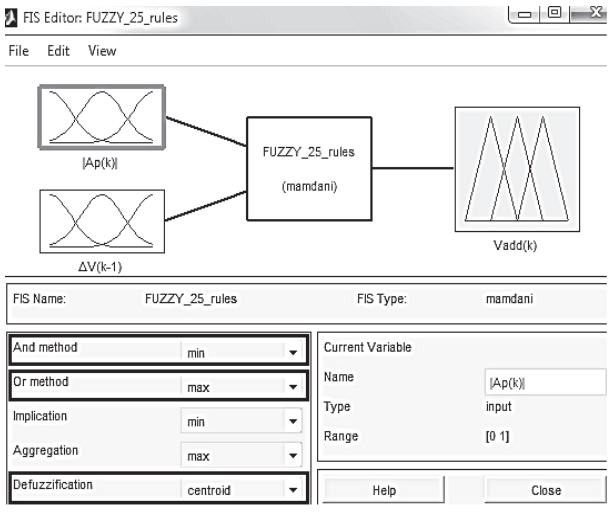

Fig. 11 Design the proposed FLC in Matlab/FIS editor.

3.2 The Second Sub-Controller

The second sub-controller is a PI controller, including an anti-windup block based on the back-calculation method [21]. Let us emphasize that the anti-windup module is used to eliminate the large overshoot in the transient response. And its detailed scheme is represented in Fig. 12.

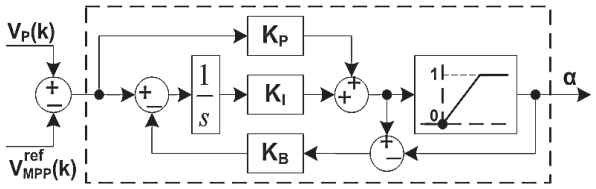

Fig. 12 The detailed scheme of the PI anti-windup in use.

4. Simulation Results

In Matlab simulations, the PV panel model is based on (1); and the closed-loop PV system is developed with the SimPowerSystems and Fuzzy Logic toolboxes [22],[23]. Design parameters of the DC-DC converter with the resistive load and the proposed fuzzy-based INC-MPPT algorithm are presented in Table 6. Additionally, let us note that the PV array consists of two parallel branches with two 80W PV panels in series in each branch; and its rated total power is 320 W.

Table 6 Design parameters of the converter and proposed algorithm.

Non-inverting buck-boost converter with load	
$C_i = C_o = 1$ mF; $R_1 = 50$ mΩ; $L_1 = 1$ mH; $R_{Load} = 15$ Ω	
Proposed algorithm	**Parameter and Value**
FLC	$g_1 = 45$; g_2: according to Table 4
PI with anti-windup	$K_P = 1.5$; $K_I = 15$; $K_B = 0.5$

Besides, the authors in [6] introduced two modified INC-MPPT techniques, using a conventional FLC and an adaptive FLC, respectively. In our research, for comparison purpose, the conventional fuzzy-based INC-MPPT technique in [6] is chosen to simulate. As shown in Fig. 13, the ratio-value ($I_P/V_P + \Delta I_P/\Delta V_P$) and its change ($dC_P$) are two inputs of the conventional FLC in this technique. The FLC's output is the change of duty-cycle value $du(k)$, where $u(k)$ plays as the input control signal of the converter. Table 7 shows design values for the input and output scaling factors of the FLC in Fig. 13. These coefficients are tuned to get a fine balance performance as possible between the fast response speed in tracking the MPP and the small steady-state fluctuation around the MPP.

4.1 *Simulation 1*: Start-up Response in Tracking the MPP at the Standard Test Condition

In this situation, the solar irradiance and the temperature are kept constant at 1000 W/m^2 and 25°C, respectively. Therein, Fig. 14 shows that the operating PV voltage V_P is equal to its desired value V_{MPP}^{ref} from the time $t = 0.1$ s (with using the proposed method). Additionally, Fig. 15 illustrates the comparison between the proposed algorithm, the conventional INC-MPPT method in [4] and the conventional fuzzy-based INC-MPPT introduced in [6].

In detail, firstly, the conventional INC-MPPT with the fixed step-size as 0.5 V (big value) has the fast response time, but includes the large overshoot and steady-state error. Otherwise,

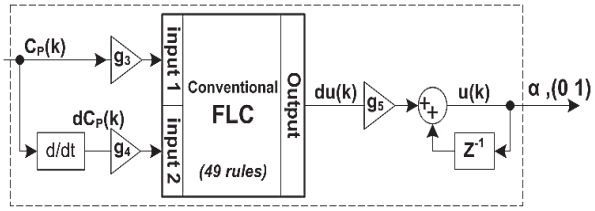

Fig. 13 The structure of the conventional fuzzy-based INC-MPPT method presented in [6].

Table 7 Input-output scaling factors of the FLC in Fig. 13.

Input scaling factors	Output scaling factor
$g_3 = 3.8$; $g_4 = 4.1$	$g_5 = 4$

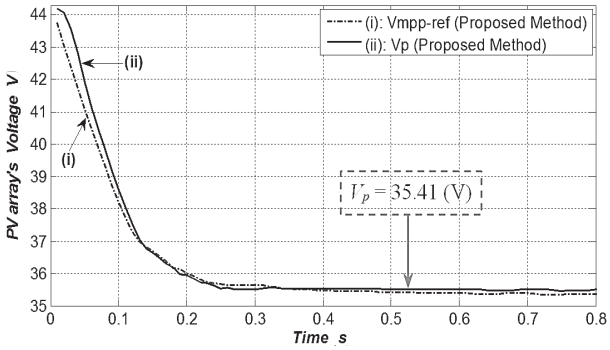

Fig. 14 The PV array's voltage in *Simulation 1*.

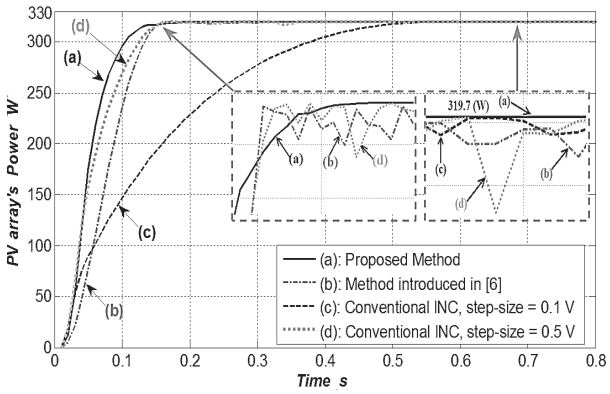

Fig. 15 The PV array's output power in *Simulation 1*.

the conventional INC-MPPT with the fixed step-size as 0.1 V (small value) has the tiny overshoot and little steady fluctuations; nevertheless, its response speed is slow. Whereas, the conventional fuzzy-based INC-MPPT in [6] can reach the MPP fairly speedily. In fact, its response is faster than the conventional INC-MPPT with fixed step-size as 0.1 V; however, variations around the MPP at the steady state have not yet been eliminated really efficiently. Lastly, the proposed method not only tracks rapidly and exactly the MPP but also significantly lowers oscillations around the MPP.

Moreover, Fig. 16 shows that the step-size $\Delta V(k)$ in the proposed technique is a variable value, and is adjusted suitably by the suggested FLC to seek the MPP efficiently. In detail, firstly, $\Delta V(k)$ has the large value as 0.7 V to reach speedily the MPP of 319.7 W. Then, its value is decreased to around 0.17 V for reducing the overshoot. Finally, it is tiny after the time $t = 0.2$s to eliminate the steady-state error.

In the next two simulations, the conventional INC-MPPT

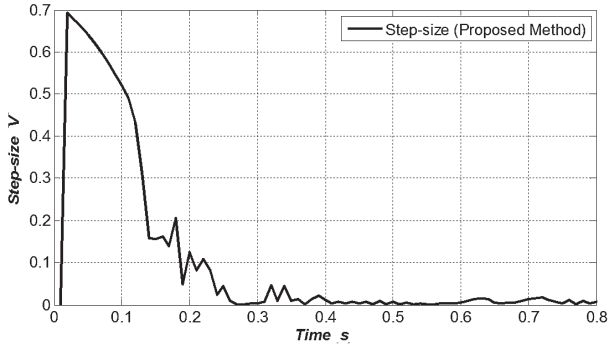

Fig. 16 The variable step-size $\Delta V(k)$ in *Simulation 1*.

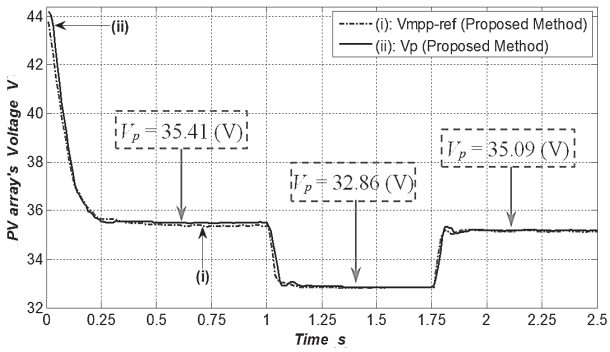

Fig. 17 The PV array's voltage in *Simulation 2*.

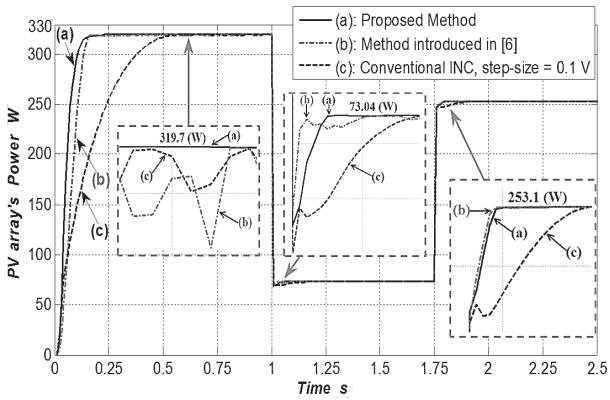

Fig. 18 The PV array's output power in *Simulation 2*.

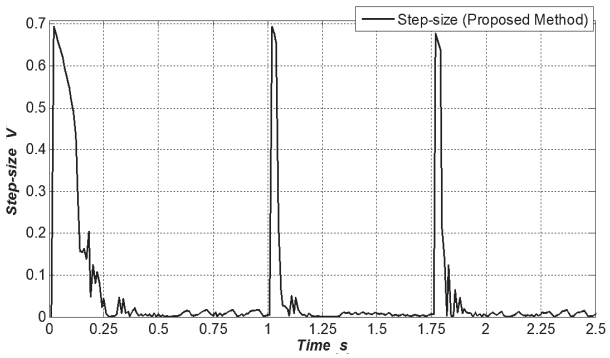

Fig. 19 The variable step-size $\Delta V(k)$ in *Simulation 2*.

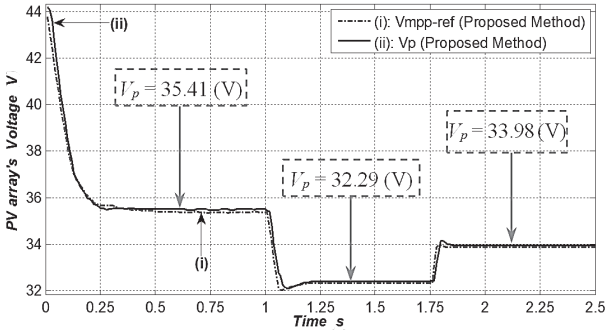

Fig. 20 The PV array's voltage in *Simulation 3*.

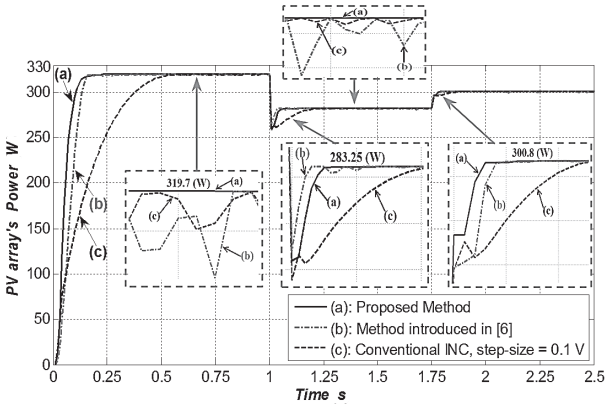

Fig. 21 The PV array's output power in *Simulation 3*.

method will be only used with the fixed step-size as 0.1 V (small value) to reduce the overshoot in transient time and steady-state oscillations around the MPP.

4.2 *Simulation 2*: Effects of Solar Radiation Changes

In this case, the solar radiation changes its value as follows: 1000 W/m^2 from the time t = 0 s, 250 W/m^2 from the time t = 1 s, and 800 W/m^2 from the time t = 1.75 s; in the meantime, the temperature is kept invariant at 25°C.

Figure 17 illustrates that the PV array's voltage V_P always closely tracks to its reference V_{MPP}^{ref} calculated by the FLC in advance. As shown in Fig. 18, the PV output power is 319.7 W, 73.04 W and 253.1 W, highly corresponding to the MPPs M3, M1 and M2 (of the PV array) seen in Table 3, respectively.

In addition, Fig. 19 represents that the step-size $\Delta V(k)$ is tuned adaptively to track the MPP quickly and exactly. In detail, when the solar radiation decreases suddenly from 1000 W/m^2 to 250 W/m^2 at the time t = 1 s, $\Delta V(k)$ is adjusted instantly from 0 V to 0.7 V to force the operating point to reach the new MPP rapidly. After that, at about the time t = 1.2 s, as the operating point is moving nearly to the MPP of 73.04 W, $\Delta V(k)$ is decreased promptly to be very small for reducing the fluctuation around the MPP. Similarly, as seen in this figure, the above process of $\Delta V(k)$ is done again when the solar irradiance increases abruptly from 250 W/m^2 to 800 W/m^2 at the time t = 1.75 s.

4.3 *Simulation 3*: Impacts of Temperature Variations

In this circumstance, the temperature varies its value as follows: 25°C from the time t = 0 s, 45°C from the time t = 1 s, and 35°C from the time t = 1.75 s; meanwhile, the solar irradiance is kept unvarying at 1000 W/m^2. With using the suggested algorithm, Figs. 20 and 21 show that the PV array operated at three power points: 35.41 V/319.7 W, 32.29 V/283.25 W, and 33.98V/300.8 W in the three operating time-periods, clearly matching the MPPs M3, M5 and M4 (of the PV array) represented in Table 3, respectively.

Besides, as described in Fig. 22, the step-size $\Delta V(k)$ is altered

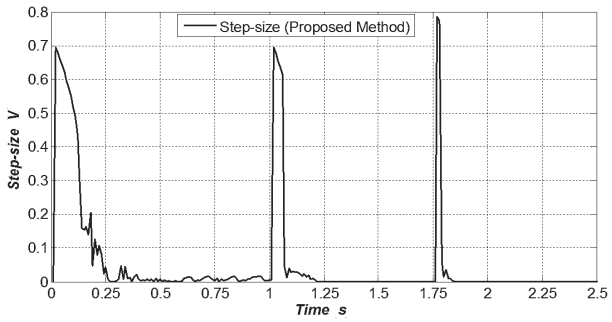

Fig. 22 The variable step-size $\Delta V(k)$ in *Simulation 3*.

appropriately to eliminate oscillations around the MPP. In detail, when the temperature changes unexpectedly its value at the time $t = 1$ s (or at $t = 1.75$ s), $\Delta V(k)$ is tuned immediately to 0.7 V (or to 0.78 V, respectively) to seek speedily the new MPP. Then, it is decreased continually to become zero.

5. Experimental Results

The experimental stand-alone PV system utilized in this study is described in Fig. 23. Therein, the PV array with a nominal power of 320W is installed on the rooftop of the Green Power Laboratory, Ho Chi Minh City University of Technology, Vietnam. The experimental non-inverting buck-boost converter is implemented according to the parameters given by Fig. 1 and Table 6. And the microcontroller board is the *Tiva C Series LaunchPad* from Texas Instruments [24]. The proposed fuzzy-based algorithm is programed in the laptop, then embedded into the microcontroller *TM4C123G* to execute in real-time. The sample time to generating the control signal α_p is $T_s = 5$ ms.

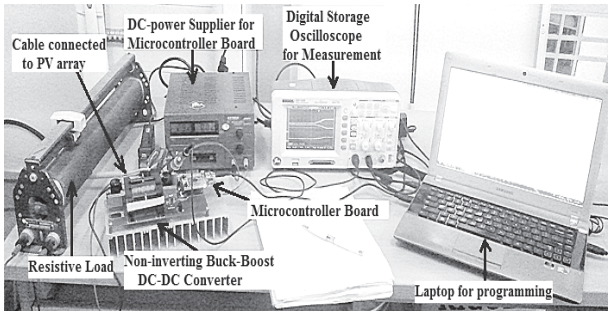

Fig. 23 The experimental PV system used in this study.

In our experiments, the solar radiation is measured as about 650 W/m^2 and the temperature on PV array's surface is nearly 42°C. As well, the performance of the proposed fuzzy-based algorithm is compared to the conventional INC-MPPT method in [4] with the fixed step-size as 0.1 V. Performances of the experimental PV system (shown in Figs. 24–26) are observed and collected with using the digital oscilloscope. In Figs. 24–26, the vertical axis (y-axis) is scales for the PV array's voltage (channel CH1), current (channel CH2) and output power (channel CHm); and the horizontal axis (x-axis) is the time scale.

5.1 *Experiment 1*: Start-Up Response in Tracking MPP

This experiment is implemented to assess the response speed in seeking the MPP of the proposed method when the PV system starts to operate. Wherein, according to Fig. 24 (a), the conventional INC reaches the MPP of 150W (30V/5A) within about 140 ms. Besides, as shown in Fig. 24 (b), the proposed

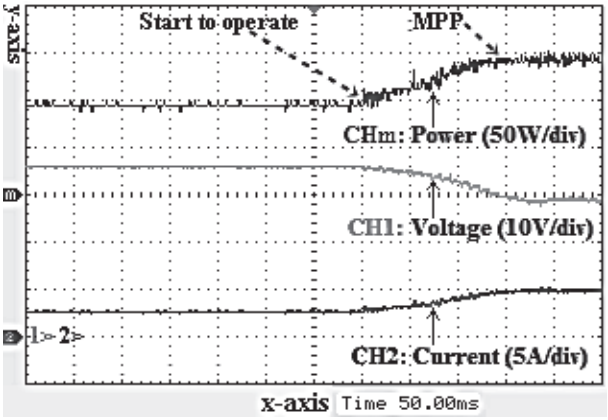

(a) With using the conventional INC-MPPT ($x-axis$: 50ms/div)

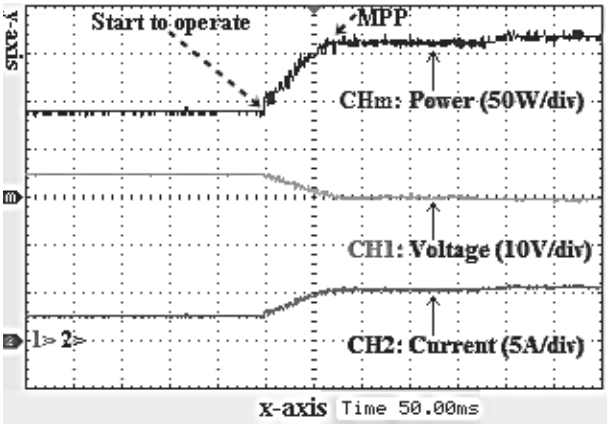

(b) With using the proposed method ($x-axis$: 50ms/div)

Fig. 24 Performances of the PV system in *Experiment 1*.

algorithm takes only 70 ms for tracking the MPP of 160W (30V/5.33A). And the above results show that the response speed of the proposed method is considerably faster than the conventional INC-MPPT method in this test.

In the next two experiments, the effectiveness and adaptability of the proposed method will be evaluated when the PV array is suddenly affected by the partial shadow effect. In detail, *Experiment 2* and *Experiment 3* are performed when the partial shadow occurs and ends, respectively.

5.2 *Experiment 2*: When the Partial Shadow Happens

Subsequent the *Experiment 1*, when PV array is operating at the power point of 180W, the surface of PV array is covered suddenly within fifty percent of its area. This means that only fifty percent of the PV array's surface is now exposed in the solar insolation. So the PV output power will decrease.

As illustrated in Fig. 25 (a), the conventional INC-MPPT takes nearly 2000 ms to search the new MPP of 100W (30V/3.33A) from the time when the partial shadow happens. Whereas, the proposed algorithm needs only 680 ms to reach the new MPP of 100W (30V/3.33A) as in Fig. 25 (b). Obviously, the suggested algorithm can seek exactly the new MPP, and it also has the better performance than the conventional INC-MPPT in this experimental circumstance.

5.3 *Experiment 3*: When the Partial Shadow Ends

Subsequent the *Experiment 2*, when the PV array is operating at the power point of about 100W, the covered surface area of it is now entirely uncovered. This means that the whole surface

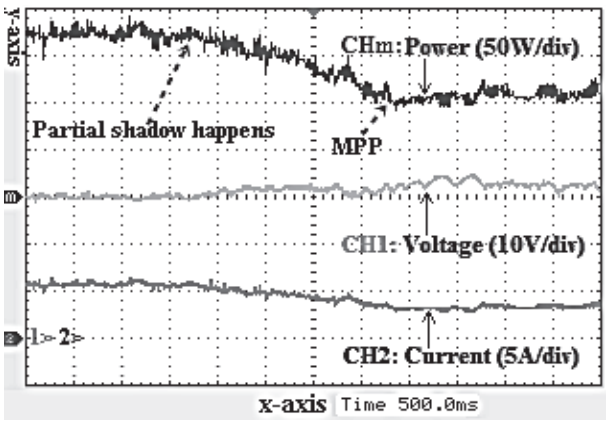

(a) With using the conventional INC-MPPT ($x-axis$: 500ms/div)

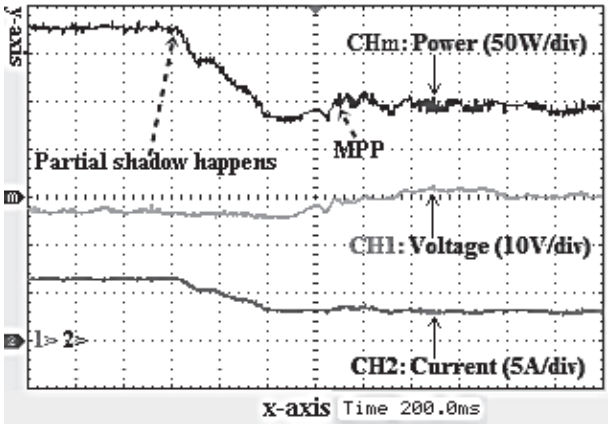

(b) With using the proposed method ($x-axis$: 200ms/div)

Fig. 25 Performances of the PV system in *Experiment 2*.

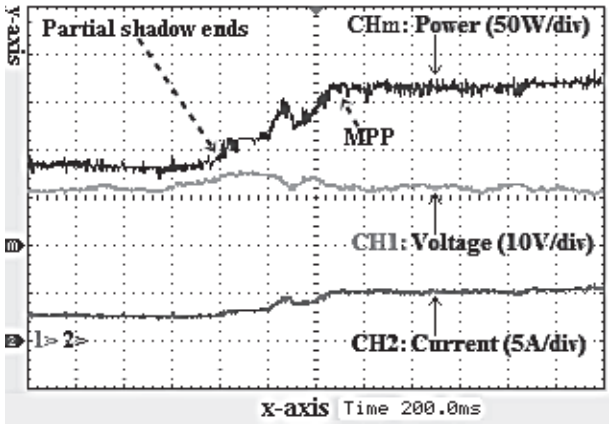

(a) With using the conventional INC-MPPT ($x-axis$: 200ms/div)

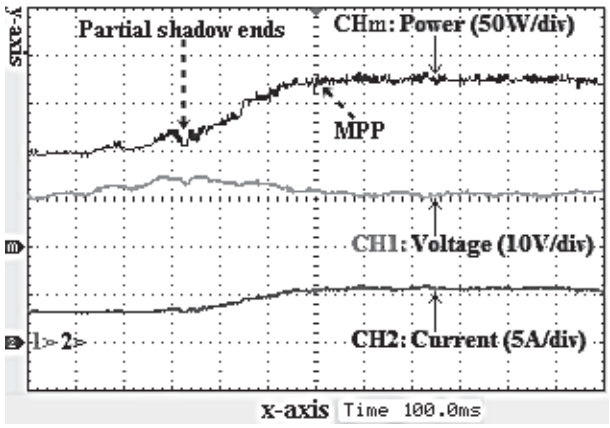

(b) With using the proposed method ($x-axis$: 100ms/div)

Fig. 26 Performances of the PV system in *Experiment 3*.

area of PV array is now exposed in the solar irradiance. Thus, the output power of PV array will increase.

In detail, as expressed in Fig. 26 (a), the conventional INC-MPPT method needs nearly 500 ms to trace the new MPP of 170W (32V/5.31A) after the partial shadow ends. While it takes 260 ms for the proposed algorithm to reach the new MPP of 175W (32V/5.47A) as seen in Fig. 26 (b). This continually demonstrates that the response speed of the suggested algorithm is always significantly quicker than the conventional INC-MPPT. And all the results obtained in *Experiment 2* and *Experiment 3* show clearly the fine adaptability of the proposed method under influences of the partial shadow.

Additionally, we can also see that the fluctuations in the PV output powers with using the proposed algorithm (shown in parts (b) of Figs. 24, 25, and 26) are pretty much smaller than the other ones with using the conventional INC-MPPT (expressed in parts (a) of Figs. 24, 25, and 26, respectively).

6. Conclusion

This paper presented a newly enhanced INC-MPPT algorithm based on fuzzy logic for stand-alone PV systems. Within the 320W stand-alone PV system for demonstration, numerical simulations obviously show that the suggested method has good performances in tracing the MPP even if the solar radiation and temperature vary abruptly. Moreover, experimental results illustrate clearly the salient efficacy of this presented algorithm even within the partial shadow case. In our next study, the proposed method will be applied to elevate the overall efficiency of the grid-connected PV systems.

Acknowledgments

Authors gratefully acknowledge Professor Ryo Watanabe (Department of Electrical Engineering and Bioscience, Waseda University) for his helpful comments on this study.

This work was partially supported by JST-CREST.

References

[1] Bader N. Alajmi, Khaled H. Ahmed, Stephen J. Finney, and Barry W. Williams: Fuzzy-logic control approach of a modified hill-climbing method for maximum power point in microgrid standalone photovoltaic system, *IEEE Transactions on Power Electronics*, Vol. 26, No. 4, pp. 1022–1030, 2011.

[2] L. Fangrui, D. Shanxu, L. Fei, L. Bangyin, and K. Yong: A variable step-size INC MPPT method for PV systems, *IEEE Transactions on Industrial Electronics*, Vol. 55, No. 7, pp. 2622–2628, 2008.

[3] K.H. Hussein and G. Zhao: Maximum photovoltaic power tracking: an algorithm for rapidly changing atmospheric conditions, *IEE Proceedings of Generation, Transmission, and Distribution*, Vol. 142, No. 1, pp. 59–64, 1995.

[4] Trishan Esram and Patrick L. Chapman: Comparison of photovoltaic array maximum power point tracking techniques, *IEEE Transactions on Energy Conversion*, Vol. 22, No. 2, pp. 439–449, 2007.

[5] Qiang Mei, Mingwei Shan, Liying Liu, Josep M. Guerrero: A novel improved variable step-size incremental- resistance MPPT method for PV systems, *IEEE Transaction on Industrial Electronics*, Vol. 58, No. 6, pp. 2427–2434, 2011.

[6] N. Patcharaprakiti and S. Premrudeepreechacharn: Maximum

power point tracking using adaptive fuzzy logic control for grid-connected photovoltaic system, *Power Engineering Society Winter Meeting*, Vol. 1, pp. 372–377, 2002.
[7] D. Menniti, A. Pinnarelli, and G. Brusco: Implementation of a novel fuzzy-logic based MPPT for grid-connected photovoltaic generation system, *Proceedings of 2011 IEEE Trondheim PowerTech*, pp. 1–7, 2011.
[8] J. Li and H. Wang: Maximum power point tracking of photovoltaic generation based on the fuzzy control method, *Proceedings of SUPERGEN 2009*, pp. 1–6, 2009.
[9] N. Khaehintung and P. Sirisuk: Application of maximum power point tracker with self-organizing fuzzy logic controller for solar-powered traffic lights, *Proceedings of 7th PEDS*, pp. 642–646, 2007.
[10] T.L. Kottas, Y.S. Boutalis, and A.D. Karlis: New maximum power point tracker for PV arrays using fuzzy controller in close cooperation with fuzzy cognitive networks, *IEEE Transaction on Energy Conversion*, Vol. 21, No. 3, pp. 793–803, 2006.
[11] A.A. Ovalle, H.R. Chamorro, and G. Ramos: Step-size fuzzy control to maximum power point tracking algorithms for PV microgrid arrays, *Proceedings of Robotics Symposium – LARC 2011*, pp. 1–6, 2011.
[12] N. Shah and R. Chudamani: Grid interactive PV system with harmonic and reactive power compensation features using a novel fuzzy logic based MPPT, *Proceedings of 7th ICIIS*, pp. 1–6, 2012.
[13] T.-F. Wu, C.-H. Yang, Y.-K. Chen, and Z.-R. Liu: Photovoltaic inverter systems with self-tuning fuzzy control based on an experimental planning method, *Proceedings of IEEE Industry Application Conference*, Vol. 3, pp. 1887–1894, 1999.
[14] H. Su and J. Bian: Maximum power point tracking algorithm based on fuzzy neural networks for photovoltaic generation system, *Proceedings of ICCASM 2010*, Vol. 1, pp. 353–357, 2010.
[15] R.F. Coelho, F. Concer, and C. Martins: A Study of the basic DC-DC converters applied in maximum power point tracking, *Proceedings of COBEP 09*, pp. 673–678, 2009.
[16] L. Zhao and Jinrong Qian: DC-DC power conversions and system design considerations for battery operated system, Texas Instruments, 2006.
[17] H. Sira-Ramírez and R. Silva-Ortigoza: *Control Design Techniques in Power Electronics Devices*, Springer, 2010 edition, 2010.
[18] M.G. Villalva, J.R. Gazoli, and E.R. Filho: Comprehensive approach to modeling and simulation of photovoltaic arrays, *IEEE Transactions on Power Electronics*, Vol. 24, No. 5, pp. 1198–1208, 2009.
[19] BP-380J 80Watt PV module, BP Solar Co., 2004.
[20] T.J. Ross: *Fuzzy Logic with Engineering Applications*, 3rd edition, Wiley, 2010.
[21] X. Li, J.-G. Park, and H.-B. Shin: Comparison and evaluation of anti-windup PI controllers, *Journal of Power Electronics*, Vol. 11, No. 1, pp. 45–50, 2011.
[22] P. Giroux, G. Sybille, C. Osorio, and S. Chandrachood: Two demonstrations of a grid-connected PV array using SimPowerSystems, *The Mathworks*, www.mathworks.com/matlabcentral/fileexchange/34752, 2012.
[23] N.G.M. Thao, M.T. Dat, T.C. Binh, and N.H. Phuc: PID-fuzzy logic hybrid controller for grid-connected photovoltaic inverters, *Proceedings of 5th IFOST*, pp. 140–144, 2010.
[24] Tiva C Series LaunchPad Evaluation Kit, Texas Instruments: http://www.ti.com/tool/ek-tm4c123gxl

Nguyen Gia Minh Thao (Student Member)

He obtained the B.Eng. and M.Eng. degrees of Electrical and Electronics Engineering from Ho Chi Minh City University of Technology (HCMUT), Vietnam, in 2009 and 2011, respectively. Since April 2009, he had became a probationary lecturer at Faculty of Electrical and Electronics Engineering, HCMUT, where he has been a Lecturer since January 2012. He is currently a Ph.D. student at Waseda University, Japan. His research interests include nonlinear control, intelligent control, and renewable-energy systems. He is a student member of SICE and ACA.

Kenko Uchida (Member, Fellow)

He received the B.S., M.S. and Dr.Eng. degrees of Electrical Engineering from Waseda University, Japan in 1971, 1973 and 1976, respectively. He is currently a Professor in the Department of Electrical Engineering and Bioscience, Waseda University, Japan. His research interests are in robust/optimization control and control problem in energy systems and biology. He is a member of SICE, ACA, IEEJ, and IEEE.

Nam Nguyen-Quang

He received the Ph.D. degree in Electronic and Electrical Engineering from the University of Sheffield, Sheffield, U.K., in 2009. He joined the Faculty of Electrical and Electronics Engineering, Ho Chi Minh City University of Technology (HCMUT), Vietnam National University, Vietnam, in 1996, where he has been a Senior Lecturer since 2012. His research interests include photovoltaic systems, soft-switching power converters, direct ac-ac power conversion, induction heating, and electromagnetic compatibility.